

First Principles Modeling of the Thermal Amine Scrubber Flight Experiment's Chemical Performance

Lawrence W. Barrett Ph.D.[1]
Jacobs JETS, Houston, Texas, 77058

The removal of atmospheric CO_2 from a spacecraft is of particular importance to NASA's mission, and is an area of continual study and technological advancement. One of the more recent advancements has been with reusable sorbents being regenerated with a combination of heat and vacuum. One such technology is the Thermal Amine Scrubber (TAS) flight experiment on the ISS, though several others are currently flying or preparing to fly. A model was created of the TAS to predict chemical performance, using fundamental chemistry and physics based on principles rather than empirical relations. Since the physical laws are true across all conditions, such a model enables greater model accuracy outside the bounds of test data, and allows for virtual testing of the hardware at conditions that are prohibitively difficult or expensive to actually test. This paper details the model's development, operation, and correlation to data from the flight unit. The model is then compared to a data set taken from the flight unit under different flow, CO_2 partial pressure, and bed configuration conditions, resulting in only a 2% error. The equations and principles laid forth in this paper are applicable to a wide range of thermally regenerated sorbents, and additional models of a similar nature would allow for potentially the most straightforward and direct method of comparison of technologies available to date.

Nomenclature

ACM	=	Aspen Custom Modeler
CO_2	=	Carbon Dioxide
ECLSS	=	Environmental Control and Life Support System
LiOH	=	Lithium Hydroxide
MPCV	=	Multi-Purpose Crew Vehicle
NASA	=	National Aeronautics and Space Administration
TAS	=	Thermal Amine Scrubber

I. Introduction

CARBON dioxide is both a product of human metabolism, and detrimental to human health. Terrestrially the health concerns resulting from direct exposure to elevated CO_2 levels are not of great concern, as the mass of CO_2 produced compared to the volume of the atmosphere allows for significant dilution while natural and artificial convection prevents pockets of CO_2 from building up to dangerous levels anywhere humans are likely to reside. NASA lists the average CO_2 concentration in 2019 as 0.31 mmHg[1]. Spaceflight is different as the vehicle has a much more limited atmosphere, resulting in a rapid buildup of CO_2 if it is not properly removed. NASA Standard 3001 limits CO_2 for nominal operations in a habitable vehicle to no more than a 1 hour average of 3 mmHg[2]. By comparison a crew of 4 can produce about 4 kg of CO_2 a day[3], which would raise the CO_2 levels in a vehicle the size of the new Orion capsule by over 150 mmHg in a day if no CO_2 is removed. For this reason CO_2 removal and sequestration has been an area of ongoing research for NASA.

Historically CO_2 was removed first with single use cartridges such as LiOH, but recent developments have focused on technologies which are not single use, particularly packed beds which undergo pressure and or temperature swings. A number of such technologies have been or will be tested on ISS either as designated ECLSS hardware or flight experiment payloads. One such flight experiment payload is the Thermal Amine Scrubber (TAS), which contains four beds of polymer beads coated with a high viscosity liquid. The liquid contains both primary and secondary amines,

[1] ECLSS Analysis Technical Lead, Thermal, Fluids and Life Support Analysis JE33, 5E307 2224 Bay Area BLVD Houston TX, 77058

which act as sites for chemisorption of CO_2, giving the coated beads the capacity to adsorb and desorb CO_2 depending on environmental conditions.

The four TAS adsorbing beds have a cycle time of about 62 minutes. The four beds are offset from each other such that a fresh bed comes online every 15.5 minutes. The cycle starts with a CO_2 uptake for 30 minutes. The bed is then equilibrated with its twin bed to save gas and begin represurising the bed at vacuum. Bed A dumps to bed B and vice versa, while beds C and D dump to each other. After the equilibrate phase, the bed undergoes an air save mode where a vacuum pump is used to pull residual air from the bed to prevent excess gas loss to vacuum. Once the air save mode is complete the bed is heated and exposed to space vacuum. The heat reduces the capacity of CO_2 on the sorbent, driving off more CO_2 than would be possible with only vacuum. The bed is allowed to cool naturally at first, and then is actively cooled while still exposed to vacuum. The active cooling provides a twofold benefit: 1) it readies the bed for adsorption as soon as it is exposed to CO_2 laden air, and 2) it protects the sorbent by preventing oxidation of the sorbent with hot air. At the end of the cooling segment, the bed receives the air dumped from its twin at the end of the twin bed's adsorption cycle, and then it reopens to accept air flow. There are always two adsorbing beds, with the exception of the moment when the beds are equilibrating and there is only a single adsorbing bed.

The TAS was in use on ISS to help control the CO_2 levels, and has proven the adsorbent is effective at CO_2 control, and is worthy of further study. As part of the study of the TAS, a fundamental model was developed in Aspen Custom Modeler (ACM), using basic scientific and physical principles. Considering the bulk of the data on the TAS has come from on board operations, the CO_2 level associated with this data is limited to that which is acceptable for long term crew exposure, and extrapolation of unit performance outside that CO_2 range cannot be supported with real data. Because the model is based on a first principles rather than empirical relationship, the model is able to more accurately predict performance outside the bounds of hardware's test dataset. This paper expounds upon the development and testing of this first principles model, and shows proof of the extrapolation capability of the model.

II. Model Basics

The model is attempting to study the thermal amine using only fundamental equations with a highly predictive nature based on known scientific laws and well established principles. For this reason the model relies heavily on the conservation of mass and energy to create a series of balances in accordance with Equation 1.

$$\Sigma(\dot{In}) - \Sigma(\dot{Out}) + Generation - Consumption = Accumulation \tag{1}$$

The model exists as a series of connected nodes, with each bed containing a number of smaller sub beds based on the real hardware configuration. Each sub bed is discretized into 20 parts, each part containing a node for the gas phase, adsorbent, and aluminum foam. Applying the mass balance to a single gas phase node x is described in Equation 2 and picture in Figure 1, where mass flows occur between the nodes upstream and downstream via both convection and diffusion, as well as a flux to the adsorbent surface.

$$\frac{\mathrm{dM}}{dt} = \dot{M}_{X-1\leftrightarrow X}^{Conv} - \dot{M}_{X\leftrightarrow X+1}^{Conv} + \dot{M}_{X-1\leftrightarrow X}^{Diff} - \dot{M}_{X\leftrightarrow X+1}^{Diff} + \dot{M}_{X}^{Surface} \tag{2}$$

$\dot{M}_{X}^{Surface}$ is the mass flux between the gas and surface phases, $\dot{M}_{i\leftrightarrow j}^{Diff}$ is the diffusive mass flow between two segments, $\dot{M}_{i\leftrightarrow j}^{Conv}$ is the convective mass flow between two connected segments, and dM/dt is the change in mass over time. Similar balances were used for each component by multiplying every term by the appropriate mass fractions. The aluminum nodes were considered inert and stationary and had no mass balance associated with them. The adsorbent mass balance was somewhat simplified, as there are no convective or diffusive terms, so the accumulation of mass is only equal to the surface to gas flux. Additionally the model assumes neither oxygen nor nitrogen adsorb on the surface, so only two component mass balances are needed, carbon dioxide and water.

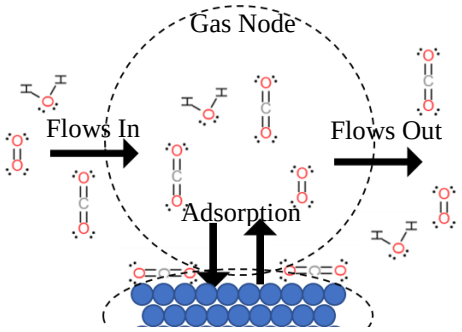

Figure 1. Graphical depiction of the gas phase mole balance

The convective terms were calculated in a circular method. The convective transfer is a function of the pressure difference between two segments based on the Ergun equation, Equation 3, the pressure in each segment is a function of the gas law, in this case the Peng Robinson Equation of State, Equation 4, the moles of gas in each phase is dictated by the mole balance, which is a function of the convective mass flow. Fortunately, ACM utilizes a simultaneous solver making it well suited to this application of iterating on a solution until convergence.

$$\frac{P_{x-1}-P_x}{L} = \frac{218.93\mu}{D_p^2}\frac{(1-\epsilon)^2}{\epsilon^3}v + \frac{4.9L\rho}{D_p}\frac{(1-\epsilon)}{\epsilon^3}v|v| \tag{3}$$

$$P = \frac{RT}{\frac{V}{n}-b} - \frac{a}{\frac{V}{n}\left(\frac{V}{n}+b\right)+b\left(\frac{V}{n}-b\right)} \tag{4}$$

In Equation 3 and Equation 4, P is the pressure, L is the length of the node, μ is the viscosity of the gas, ε is the void fraction, *v* is the superficial velocity, D_p is the adsorbent bead diameter, R is the universal gas constant, V is the node volume, n is the moles in the gas phase of the node, a and b are parameters that are calculated from specific component properties. In the Ergun Equation, the traditional constants of 150 for the flow term and 1.75 for the inertial term have been adjusted to better fit the data.

The diffusive mass transfer terms were calculated using Fick's law of diffusion, Equation 5, where j is the flux on a mass/min/unit area basis, A is the cross sectional area through which diffusion is occurring and is a function of bed geometry, $\mathcal{D}$ is the diffusivity of the components and is calculated from ACM's internal data library, C is the concentration of the species in the node, and dx is the distance between the nodes, equal to 1/20 the bed length. No diffusion is assumed on the inlet and outlet of the beds, only within the bed.

$$\dot{M}_{X-1\leftrightarrow X}^{Diff} = A * J_{X-1\leftrightarrow X} = A * (-\mathcal{D}) * \frac{(C_X - C_{X-1})}{dX} \tag{5}$$

Note that diffusive mass transfer is of little practical value during adsorption as the convective term is far greater, but after the bed has been emptied diffusion becomes the primary transfer mechanism. The last portion of the mass balance equation is also the most complex and important for the operation of the model, the flux of material onto the surface, and is described in Equation 6, visualized in Figure 2.

$$\dot{M}_X^{Surface} = M_{Adsorbent} * k_{c_i} * \left[\frac{6*(1-\epsilon)*Kg_i}{D_p\rho_{bulk}}\right] * \left(C_i^{Real} - C_i^{EQ}\right) \tag{6}$$

The terms are as follows: $M_{Adsorbent}$ is the mass of adsorbent in the node, k_{ci} is a fit parameter used to match the model to test data, K_{gi} is the mass transfer coefficient calculated by using the Reynolds number Equation 7 and either the Wakao, Equation 8, or Wilson, Equation 9, relationship, ρ_{bulk} is the bulk density of the adsorbent, C_i^{Real} is the real gas phase concentration, and C_i^{EQ} is the equilibrium gas phase concentration that would be expected based on the isotherms and current loading of species i on the surface of the adsorbent bead. The difference between the two concentrations, what the gas phase has and what the solid phase wants the gas phase to have, provides a driving force capable of adsorption, right side of Figure 2, and desorption, left side of Figure 2, depending if the surface wants to be cleaner or more heavily laden. The bracketed portion of the equation acts as the kinetic rate term to determine how fast the transfer takes place as a function of the adsorbent particles and flow parameters. Combined the rate term and the concentration difference act as a surface flux normalized to the mass of adsorbent present, which is why the total rate for a node is this flux multiplied by the mass of adsorbent present in the node.

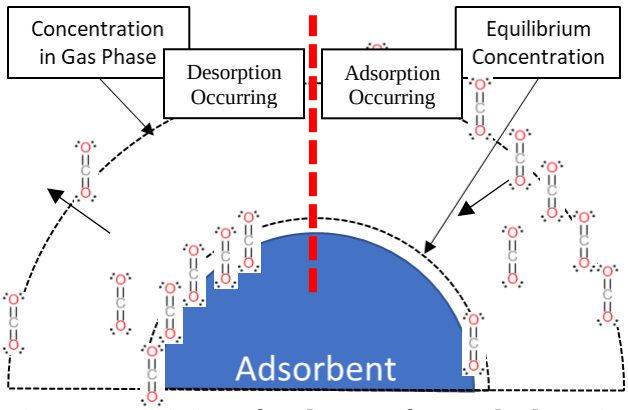

Figure 2. Depiction of sorbent surface and adsorption (right) and desorption (left) process

$$Re = \frac{\rho|v|D_p}{\mu(1-\epsilon)} \tag{7}$$

RE>3 $$K_{g_I} = \frac{\mathcal{D}}{D_p} * (2 + 1.1 * Re^{0.6} Sc^{.33}) \tag{8}$$

RE>3 $$K_{g_i} = \frac{\mathcal{D}}{D_p}\left(\frac{1.09}{\epsilon} * Re^{0.33} * Sc^{0.33}\right) \tag{9}$$

In Equations 7-9, all terms described are the same as above and Sc is the Schmidt number described in Equation 10.

$$Sc = \frac{\mu}{\rho * \mathcal{D}} \tag{10}$$

The last remaining piece of the puzzle for the mass balance is the isotherms used to calculate the concentration of the gas in equilibrium with the surface. Water uses the Fruendlich isotherm described in Equation 11with a single fit parameter α and the relative humidity, RH, while carbon dioxide uses the Toth isotherm Equation 12 and uses three fit parameters, α, β, and τ.

$$Q_{eq} = \alpha * RH^2 \tag{11}$$

$$Q_{eq} = \frac{\alpha * C_i^{EQ}}{\left(1+\left(\beta * C_i^{EQ}\right)^{\tau}\right)^{\frac{1}{\tau}}} \tag{12}$$

The energy balances were also applied to the governing conservation balance. It was assumed that heating and cooling was applied to the outside of the beds and only transferred to the beds through the aluminum foam. Heat transfer in the model occurs through all three methods, convection, conduction, and radiation. Additionally, heat transfer occurs between the aluminum foam and the adsorbent beads, the aluminum foam and the gas, and the adsorbent beads and the gas, leading to an energy balance that contains more equations than the mass balance, but given the simplicity of the heat transfer is overall less complex. The energy balance for a single node of aluminum foam is shown below Equation 13.

$$MC_p \frac{dT}{dt} = Q_{Al}^{Rad} + Q_{Adsorbent}^{Rad} + Q_{Al\leftrightarrow Gas}^{Conv} + Q_{Al\leftrightarrow Adsorbent}^{Conv} + Q_{Al\leftrightarrow Adsorbent}^{Cond} + Q_{Al\leftrightarrow Al}^{Cond} + Q^{Heater} \tag{13}$$

M is the mass of material in the node, C_p is the heat capacity of the material, dT/dt is the change of temperature over time, Q refers to heat transfer rates, superscript Rad is radiation, superscript Cond is conduction, superscript Conv is convection, and the subscript refers to what two nodes the heat is being transferred between. The Q^{Heater} term refers to external heat flux either in or out based on the heater and coolant to the thermal cycling, which only exists in the energy balance for the aluminum foam. The energy balance for the solid and gas phase also includes the heat of adsorption term, which is the heat of reaction for the adsorbing species multiplied by the molar rate of flux to the surface calculated from Equation 6. The conduction with the adsorbent term becomes complicated, as there is minimal contact between the beads and other surfaces. Due to the aluminum foam providing structure, and the bed existing in microgravity, there is little force to press the granules together as there is in a terrestrial packed bed. During adsorption and the bed evacuation, it can be assumed there is sufficient air flow for drag to press the adsorbent beads gently against each other, while during the majority of the desorption cycle conduction disappears and radiation dominates the heat transfer mechanism.

III. Testing of the Model

A. Comparing the model to expected theoretical results

Prior to any data fit or comparison, the model was evaluated subjectively to determine if certain key parameters were behaving as expected. Specifically the bed gas phase CO_2, bed CO_2 loading on the adsorbent, and temperature were evaluated as a function of time on stream to ensure the dynamic and time dependent equations were behaving as expected. The actual magnitude of each parameter in this evaluation was not considered important, only the overall behavior. Results can be seen in Figures 3-5.

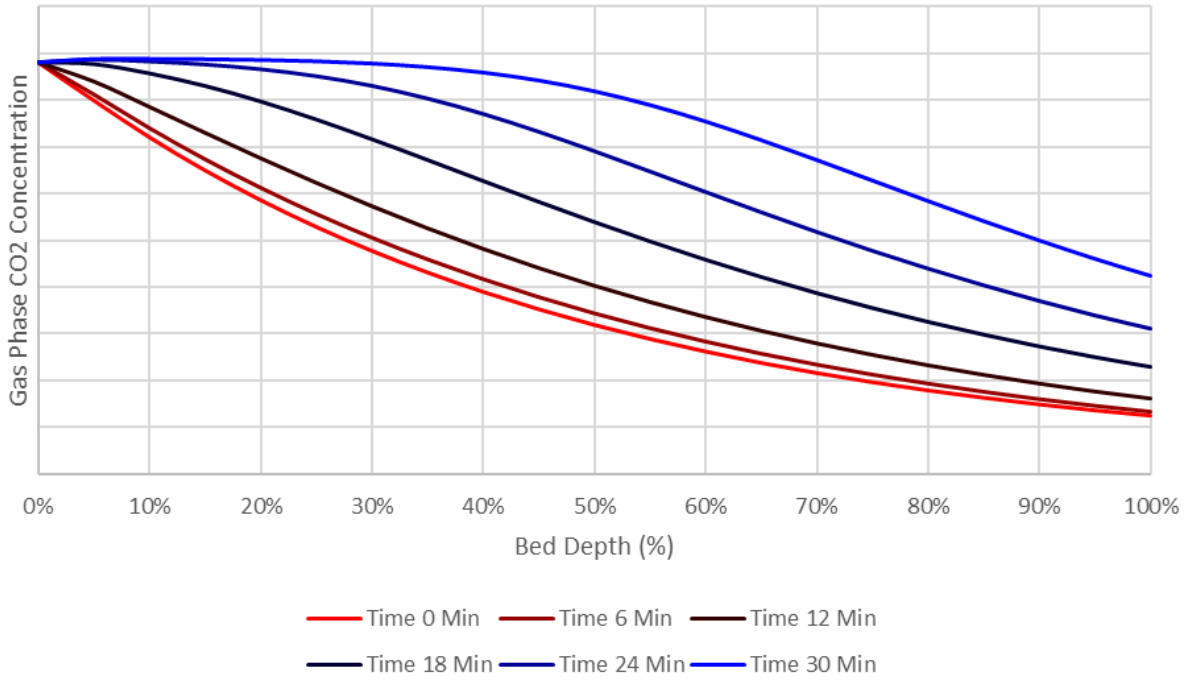

Figure 3. Gas phase molar CO_2 concentration as a function of bed depth and time on stream.

As can be seen in Figure 3, at the start of a half cycle the bed's CO_2 concentration exhibits the classic exponential decay of adsorption on a fresh bed, the concentration at the inlet is high and as the gas proceeds deeper and deeper into the bed more of the CO_2 is lost to the surface. The bed is not deep enough to reach a true asymptote, but it can be seen how such a limit likely exists, which corresponds to the isotherm for CO_2, and what is the gas phase concentration at some minimum loading. As time progresses, the front of the bed approaches saturation of CO_2, and adsorption is slowed, allowing the CO_2 concentration to stay high until deeper into the bed. This corresponds to a slight rise in the outlet concentration. Finally near the end of the half cycle, the inlet is at saturation and no adsorption occurs until a set bed depth. This corresponds to a substantive rise in the outlet concentration, as the portion of the bed available for adsorption has effectively become shorter. This behavior is expected, though the exact outlet concentration will still need to be matched to the data, and is shown in section III B.

Figure 4 shows the CO_2 loading on the adsorbent within the bed, and demonstrates the inverse of Figure 3. At the start of adsorption, the front of the bed is quickly and heavily laden, while nodes deeper in the bed see a lower gas phase concentration and therefore adsorb less. As the time on stream progresses the front of the bed approaches EQ, at which point the adsorption slows down at the front, and is more substantial at the midpoint and end of the bed. Eventually both the front and middle of the bed are nearly saturated and substantial adsorption only occurs near the end of the bed. Note the midpoint does not appear to be reaching the same equilibrium point as the front of the bed due to temperature effects discussed below. During desorption the loading quickly reaches a minimum value.

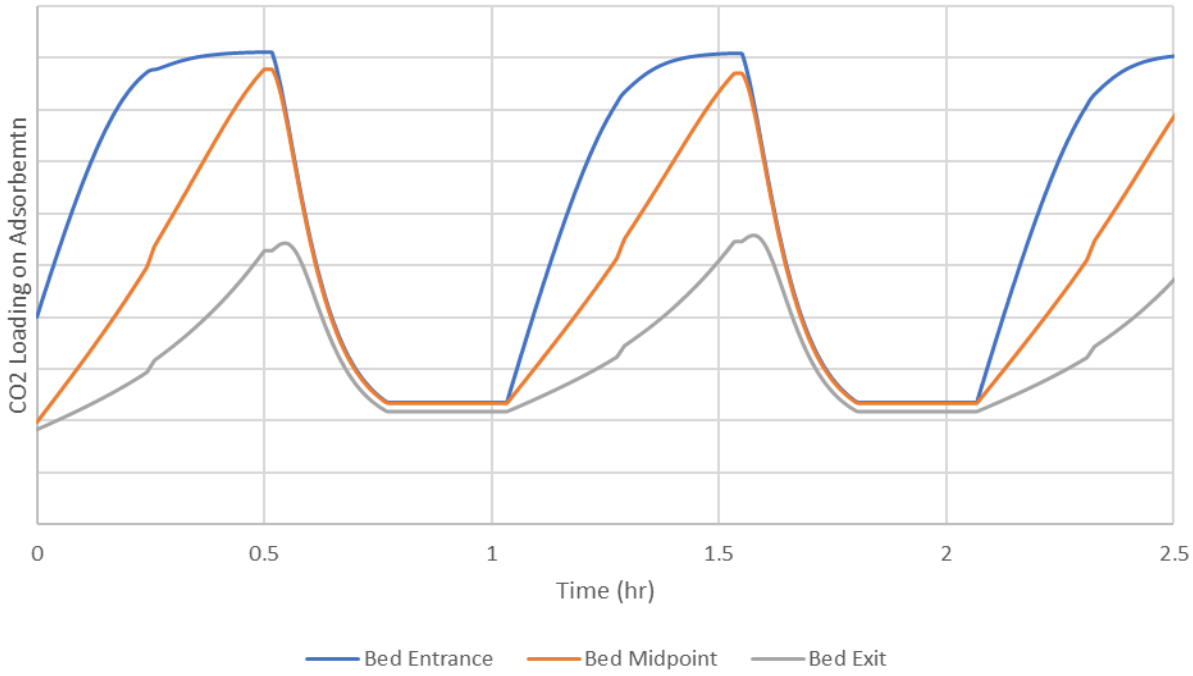

Figure 4. Bed CO_2 loading as a function of time on stream for three nodes within the model, at the entrance, midpoint, and exit of the bed.

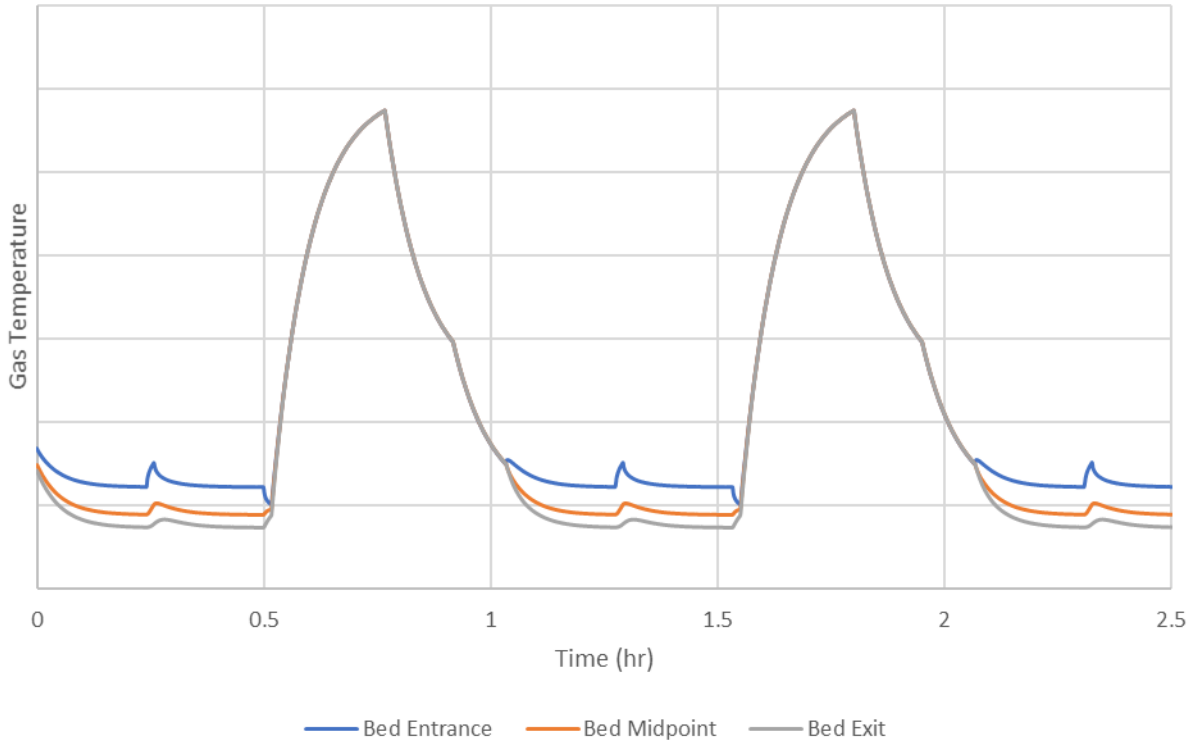

Figure 5. Temperature profile of the gas within the bed as a function of time on stream

The bed is being actively cooled during desorption to a point a few degrees below in inlet gas temperature. As a result the inlet to the bed is slightly warmer than the exit to the bed, as the gas loses heat as it passes over the cooled aluminum and adsorbent. A temporary blip in the adsorption cycle can be seen as when the second adsorbing bed begins to equilibrate pressure with its twin, before the twin comes back online for adsorption. During this time the gas velocity is increased dramatically, leading to more room temperature air flow in the system and slightly warmer temperatures. Once the flow is stopped and the bed is being heated, the metal to metal conduction of the aluminum foam nodes to the adjacent nodes dominates over the convective heat transfer to make the bed nearly uniform in temperature. The heat added was sufficient to reach the set point temperature just prior to the hot desorption phase changed to the neutral desorption phase. Each of the three desorption phases are clearly visible on the temperature graph, each with their own sudden change. The temperature is not exactly isotherm prior to adsorption. Unfortunately data on the internal bed temperatures was not available during the development of this model, but overall the trends observed are similar to what is expected and the temperatures seem reasonable.

B. Fitting the model to flight data

The model was first fit to a 12 hour section of flight data from ISS by modifying the k_c term for CO_2 from Equation 6. This flight data was from nominal operations, with all 4 beds. The module CO_2 concentration and TAS outlet concentration were used to find a difference in CO_2 upstream and downstream of the TAS unit. This was slightly misleading as the module concentration is only taken every 45 minutes, while the outlet concentration is nearly continuous, leading to uncertainty in the actual concentration difference. The fan speed was used with the fan curve to determine a flow rate, and with the concentration difference a removal rate for CO_2 was calculated. The model was given the same inlet concentration and flow rate as a function of time and the total removal rate calculated, and can be seen below in Figure 6, with a total difference over the day of less than 1%.

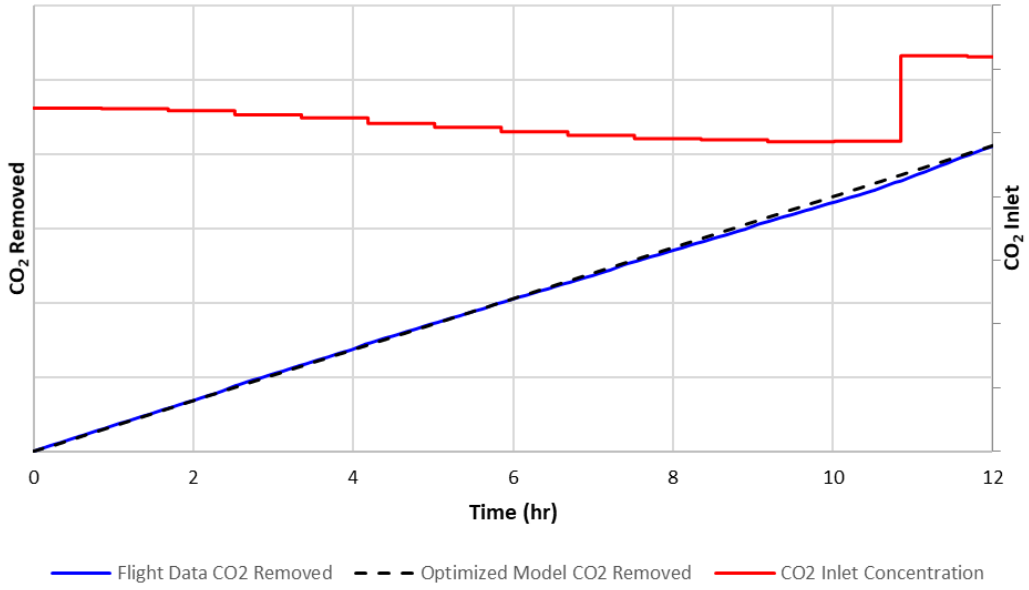

Figure 6. TAS model vs flight performance for a 12 hour period.

The fit model using the same constants was applied to a full week of data to determine how the model might fair when inlet conditions varied more than for the short fitting period. After a full week, the difference between the model and the flight unit was still less than 1% deviation aslong as the inlet concentration and flow rate from the flight data were input to the model. This shows the fit parameters are good over the ideal operating range, though neither the flow nor the inlet concentration strayed significantly outside the bounds of the data set for the 12 hour fit. The comparison can be seen below in Figure 7.

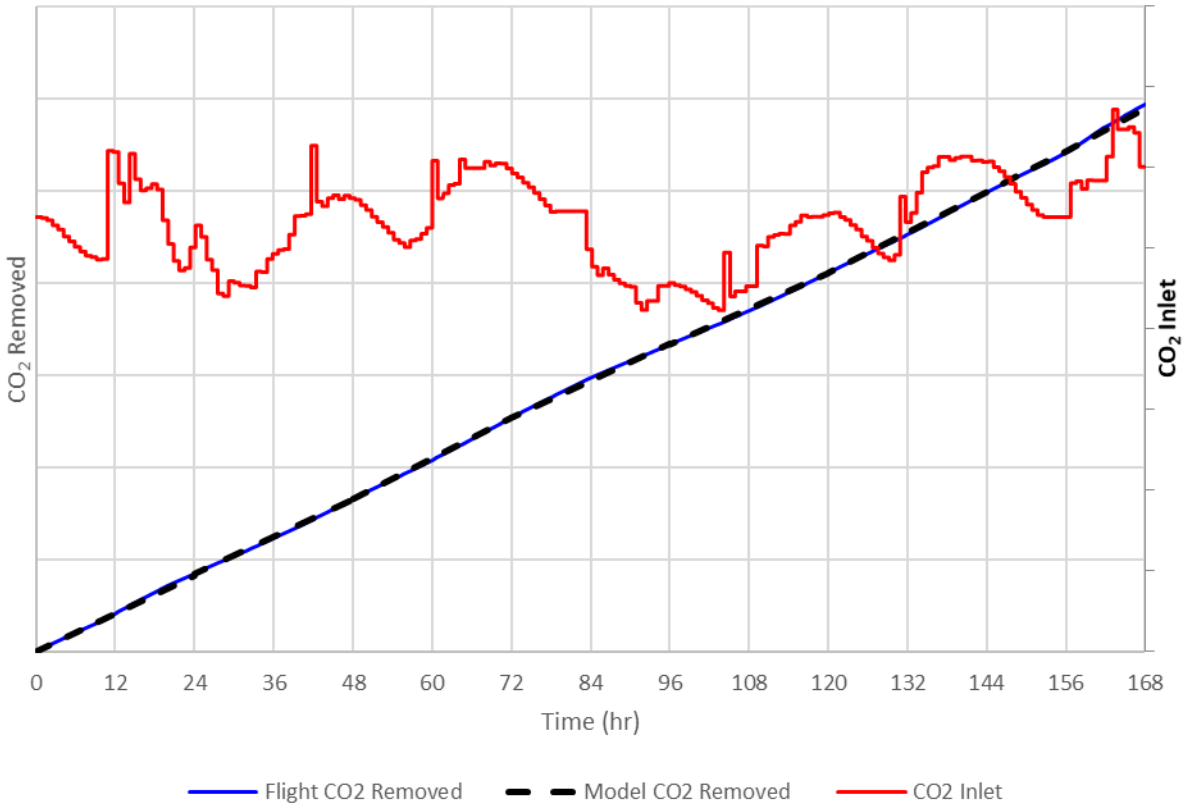

Figure 7. Week long data fit between TAS model and flight unit

C. Extrapolating on the model

Sometime after the initial model fit, the flight unit was upgraded to include an inlet CO_2 sensor with more frequent data readings than the 45 minute node CO_2 readings. Additionally, the flight unit was operating in a different configuration, with only two beds operating and a corresponding lower flow rate. As a result of this lowered performance, other unspecified CO_2 systems were active and the overall ISS CO_2 level was lower than the initial analysis. Since the flow rate, bed configuration, and inlet concentration had all changed, this was deemed an appropriate period of time to evaluate how well the model could extrapolate TAS performance from its originally fitted dataset. The results can be seen below in Figure 8. It is worth noting the numbers have been stripped from the axis for data control purposes, but the total magnitude of the CO_2 Inlet concentration axis for Figure 7 and Figure 8 are identical to allow comparison. As can be seen, there is a slight overshoot in the model prediction, though with less than 2% deviation from the flight data, the extrapolation of the model is still considered successful. This shows the fundamental nature of the TAS allows for significantly more flexibility and use of this model than an empirical model might.

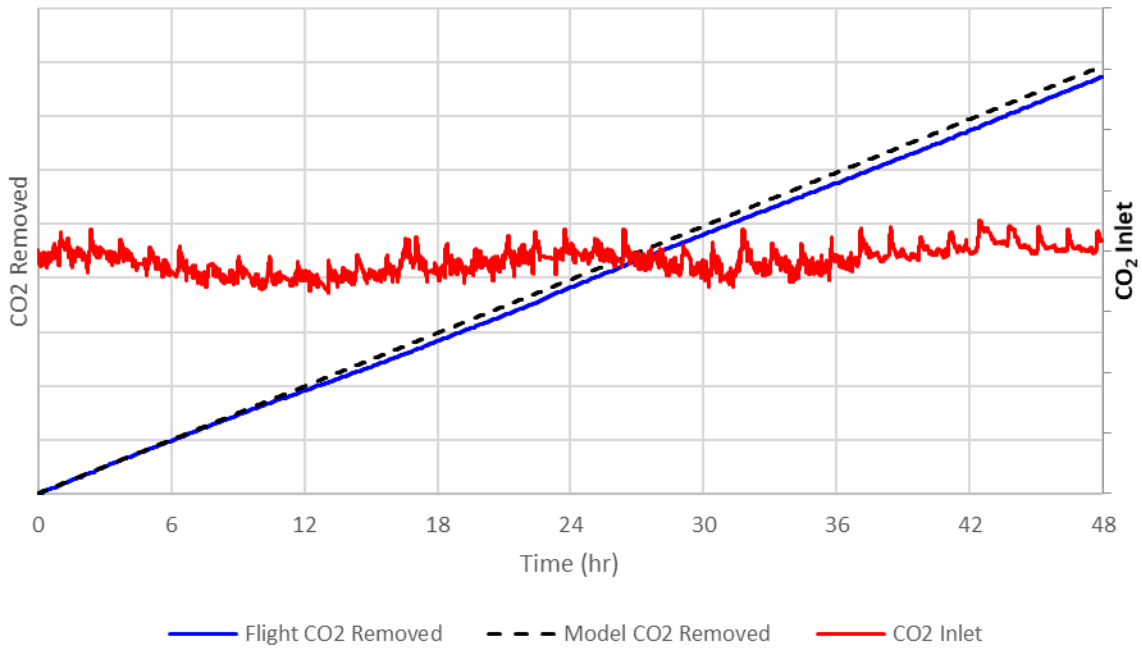

Figure 8. Total CO_2 removal matching flight unit TAS with the model, showing good data extrapolation capability.

IV. Conclusions

A model of the TAS unit's performance was designed from a fundamental first principles standpoint such that a wide range of operational conditions could be analyzed. The flight unit was used first to validate the model and fit certain kinetic parameters, and then as a testing ground to see if the model could be given real inputs from ISS and predict the performance under both similar and dissimilar conditions to which the model was fit. The model was able to match the ISS data to within 1% of the CO_2 removed for periods of operation that were within the bound of the fit dataset, and within 2% when extrapolating on conditions outside the fit dataset. This shows the robust nature of a fundamental model, as long as the physics of the hardware are properly captured, then the model will have good agreement with test data. The model has already been integrated into larger air revitalization architectures for integrated analysis of the TAS under a wide range of operating conditions. Future work is planned to combine the model with a CO_2 reduction model such as the Sabatier to evaluate potential closed loop operations onboard both ISS and the Gateway.

V. References

[1] Buis, A. (2019, October 9). *NASA's Jet Propulsion Laboratory*. Retrieved from NASA.gov: https://climate.nasa.gov/news/2915/the-atmosphere-getting-a-handle-on-carbon-dioxide/#:~:text=The%20concentration%20of%20carbon%20dioxide,it%20was%20near%20370%20ppm.

[2] Polk, J. D. (2022, April 8). NASA Space Flight Human System Standard. NASA

[3] Board, G. P. (2021, March 18). Gateway subsystem specificaiton for the environmental control and life support subsystems (ECLSS). *GP 10004*. Houston, Texas, United States of America: NASA.